Dyna
ISSN: 0012-7353
dyna@unalmed.edu.co
Universidad Nacional de Colombia
Colombia

MÚNERA, NATALIA; LORA, GABRIEL J.; GARCIA-SUCERQUIA, JORGE
EVALUATION OF FRINGE PROJECTION AND LASER SCANNING FOR 3D RECONSTRUCTION OF DENTAL PIECES
Dyna, vol. 79, núm. 171, febrero, 2012, pp. 65-73
Universidad Nacional de Colombia
Medellín, Colombia

EVALUATION OF FRINGE PROJECTION AND LASER SCANNING FOR 3D RECONSTRUCTION OF DENTAL PIECES

EVALUACIÓN DE PROYECCIÓN DE FRANJAS Y ESCANEO LÁSER PARA LA RECONSTRUCCIÓN 3D DE PIEZAS DENTALES

NATALIA MÚNERA

Physics Eng, Escuela de Física, Universidad Nacional de Colombia Sede Medellín, nmunerao@gmail.com

GABRIEL J. LORA

Physics Eng, Escuela de Física, Universidad Nacional de Colombia Sede Medellín, gjloraj@gmail.com

JORGE GARCIA-SUCERQUIA

PhD Physics, Escuela de Física, Universidad Nacional de Colombia Sede Medellín, jigarcia@unal.edu.co

Received for review March 3 th, 2010, accepted April 11th, 2011, final version April, 29th, 2011

ABSTRACT: The rapid prototyping and copying of real 3D objects play a key role in some industries. Both applications rely on the generation of appropriated computer aided manufacturing (CAM) files. These files represent a set of coordinates of an object and can be understood by a computer numerically controlled (CNC) machine. Non-contact techniques, like laser scanning and fringe projection, are among the possibilities for obtaining such CAM files. In this work, a comparison between the two aforementioned non-contact techniques is presented. The comparison is made based on their performance as candidates for generating CAM files of objects of high reflectivity and maximum lateral dimensions of the order of 15 mm The parameters tested are the quality of the 3D reconstruction, the processing time, and the possibility of these being implemented in industrial scenarios, among others. Under the scope of these parameters, it is concluded that laser scanning offers superior performance for the kind of objects here considered. The techniques are evaluated with dental pieces in order to validate these methodologies in the rapid prototyping and copying of teeth.

KEYWORDS: fringe projection, laser scanner, 3D reconstruction

RESUMEN: La generación rápida de prototipos y la copia de objetos 3D reales desempeñan un papel clave en algunas industrias. Ambas aplicaciones se basan en la producción de archivos apropiados de fabricación asistida por computadora (CAM). Estos archivos representan un conjunto de coordenadas del objeto y que pueden ser entendidos por máquinas de control numérico (CNC). Técnicas de no contacto, como el escaneo láser y la proyección de franjas, se cuentan entre las posibilidades de generar los archivos CAM. En este trabajo se presenta una comparación entre las dos mencionadas técnicas de no contacto, sobre la base de su desempeño como candidatos para la generación de archivos CAM de objetos con dimensiones laterales máximas del orden de 15 mm y alta reflectividad. Los parámetros de prueba son la calidad de la reconstrucción 3D, el tiempo de procesamiento, la posibilidad de ser aplicado en los escenarios industriales, entre otros. En el marco de aplicación de estos parámetros se concluye que el escaneo láser ofrece un rendimiento superior para el tipo de objetos aquí considerados. Las técnicas son evaluadas con piezas dentales para la validación de estas metodologías en la generación rápida de prototipos y copiado de dientes.

PALABRAS CLAVE: proyección de franjas, escaneo láser, reconstrucción 3D

1. INTRODUCTION

Dimensional control and rapid prototyping are needed in many industries. These techniques are supported on the possibility of generating a 3D representation of the objects of interest. The best case scenario is the possibility of obtaining 3D reconstruction without any mechanical contact and in the shortest possible time. Optical metrology techniques offer a solution for these requirements. These optical methods can be divided into two large categories: interferometric and non-interferometric. Although both approaches can generate a 3D representation of an object, they have specific ranges of application and sensitivity. Because the objects of our interest (dental pieces) are in the range of application of the non-interferometric methods, we only introduce the reader to this type of optical methodology.

There are several non-interferometric methods used to produce a 3D representation of an object. These include:

time/light in flight, moirè, photogrammetry, laser scanning, and fringe projection, among others [1]. As its name indicates, the time/light in flight technique measures the time difference that a light source undergoes as it travels on two different paths. One path is of a known length, and therefore the time difference can be converted in a distance [2]. The time difference is computed for each of the points of the object and then a 3D *time differences set* of the object is generated. The sensitivity of the method is of the order of millimeters. To improve this sensitivity, different techniques avoid the direct measurement of the time difference: some use image correlation [3] and/or by holography methods that employ sources with reduced temporal coherence [4–6].

One widely applied method for 3D reconstruction of objects is the moirè effect. This phenomenon occurs as two regular patterns are superimposed over a surface. Its use in optical metrology started in the 1920s with the work of Ronchi [7], Raman [8], and Datta [9]. The moirè effect has been used in fields as diverse a life science and engineering. In life sciences, moirè has provided valuable information in facial plastic surgery [10], in the study of vertebral column malformations [11], and in face morphometry [12], among many others. The study of strain and stress of materials [13], the measurement of the deformation of a bridge [14], are some examples of the use of the moirè technique in engineering. The use of moirè in the mapping of phase objects and mirror-like surfaces [15,16] should also be named.

Another method to generate a digital 3D representation of an object is the photogrammetry technique. This method determines the geometrical properties of an object through a series of photographic images [17]. The method has been improved by the use of two or more photographic images taken from different positions; the common points are identified on each image to obtain the required information. The intersection of the *known rays* originated at the different camera position can determine the 3D points that constitute the object [18,19].

Perhaps the simplest and most used methods for 3D reconstruction of objects are laser scanning and fringe projection. In laser scanning, one uses the method of optical triangulation [20] to reconstruct the 3D object. In this method, a laser line is projected on a reference surface and the object under study. The comparison of the absolute positions of both lines on the plane of the recording device provides the 3D information of the object via a map of heights. The use of structure light [21], the projection of simultaneous multiple stripe [22], the use of hand-held laser and standard grayscale cameras [23] are methods proposed for improving the performance of laser scanning.

The other widely used method for 3D reconstruction is fringe projection. This methodology encodes the depth information via the deformation that suffers a known fringe pattern. The deformed pattern is recorded with a digital sensor, and the fringe deformation is analyzed via conventional methods of phase extraction [24–26]. The very portable, reliable, and cheap digital devices for fringe projection and their recording (which are available on the market) have propelled the wide use of this methodology for 3D reconstruction. The analysis of the fringes is performed on very fast personal computers, and systems operating in real time can provide accurate 3D reconstruction of the object under study [27].

Since all the above techniques use light as a probe, they are of great interest for obtaining the 3D reconstruction of an object. They do not destroy the samples at the time of analysis, which ensures that the object will not be distorted by the measuring technique. The surfaces generated are used in applications such as reconstructive surgeries [28], the documentation of archeological or architectural pieces [29], security applications [30], in forensic science [31], dentistry [32], reverse engineering [33], and many other production fields [34,35].

Because of their accuracy, robustness, simplicity and possibility of being implemented in industrial environments, we present a comparison between fringe projection and laser scanning techniques for 3D reconstruction of dental pieces. These pieces, whose lateral dimensions are in the range of 5mm to 15mm, have surfaces with high reflectivity which makes the measuring process more difficult. The paper is organized as follows: in Section 2 we present a brief introduction to both techniques. In Section 3, the comparison of the experimental performance of both methods is shown and we present some conclusions in Section 4.

2. TECHNIQUES DESCRIPTION

2.1 Fringe projection

In fringe projection, a fringe pattern which could be cosine- or Ronchi-type, is projected on a reference plane and thereafter over the object under study. The two independently recorded images of the fringes are saved for

their analysis. The assessment of the differences between these records is the core of the fringe projection technique; currently it is performed by digital means providing great versatility and speed of performance. Figure 1 illustrates the fringe projection technique. For providing even more versatility and speed to the technique, the fringe patterns are generated in a personal computer (PC) and projected using a commercial liquid crystal display (LCD). A charge-coupled device (CCD) camera is used for imaging and recording the projected fringe patterns; the recorded images are sent to a PC for their processing where the 3D representation of the object is produced.

In general, a fringe pattern with a period dx is projected perpendicularly onto a reference plane and onto the object studied. The latter is represented by the S curvature in Fig. 2. Due to the presence of the object, the fringe located at the point P1 on the reference plane undergoes a displacement towards P2. This shift is related with the geometrical setup:

$$u(x) = z \tan\theta \qquad (1)$$

with z representing the distance from the reference plane to the surface of interest, θ the angle between the projection and viewing directions, and u(x) the lateral displacement of the fringe analyzed on the reference plane.

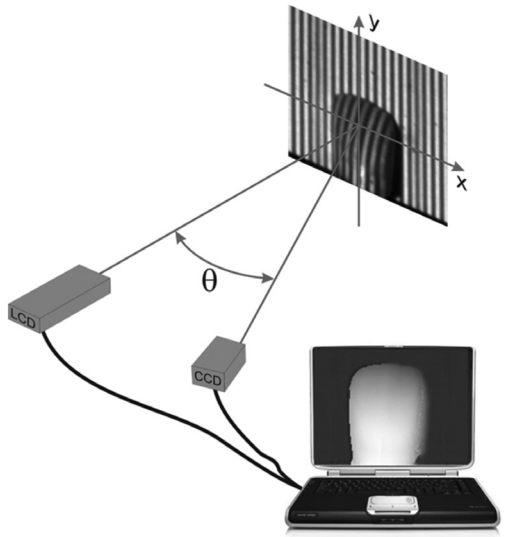

Figure. 1. Illustration of a fringe projection system. The fringe pattern generated in the PC is projected by the LCD. The CCD camera records the fringe patterns projected on the reference and object surfaces.

If the projected fringes are cosine-type, the displacement of the fringe pattern will be noticed in a change in the argument of the function; namely, it changes phase $\psi(x)$. This phase shift is related to the fringe pattern period by $\psi(x) = 2\pi u(x)/d_x$. The value z for each of the x values can be found through the assessment of phase $\psi(x)$ of the deformed fringe system evaluated at the point of interest x [36]:

$$z(x) = \frac{d_x}{2\pi \tan\theta}\psi(x). \qquad (2)$$

According to Eq. (2) the correct finding of the height map $z(x)$ relies on the appropriate measurement of the phase map $\psi(x)$. In the literature there are various methods for finding phase $\psi(x)$—the Fourier transform method [37] or any of the phase shifting techniques [38] are the most efficient and widely used. Once phase $\psi(x)$ is obtained, the height map $z(x)$ can be obtained, thus the topography of the surface of the studied object is reproduced. The 1D analysis here presented can be straightforwardly extended to 2D, leading to the map of heights $z(x,y)$ that constitutes the topographical representation of the object under study, namely its 3D reconstruction.

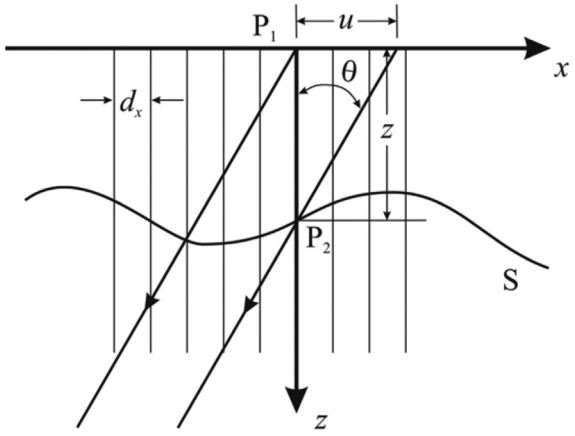

Figure 2. Fringe projection geometry on an arbitrary surface with regard to the reference plane. θ is the angle between the projection and viewing directions.

2.2 Laser scanning

In laser scanning, a laser spot is used as a sampling tool of the surface to study. An imaging system captures an image of the laser spot on the detector plane. Conventionally the detector is a CCD camera which has been previously calibrated. The optical

axis of the imaging system makes an angle θ_2 with respect to the perpendicular at the reference plane. The laser beam makes an angle θ_1 with respect to the same perpendicular, as shown in Fig. 3. In the same way as it is for fringe projection, initially the spot is projected onto a reference plane. The image of the spot for each position is recorded, such that the corresponding location of that image on the detector is registered as zero height; this process constitutes the initial calibration step of the CCD [23]. The information on the height with respect to the reference plane is therefore given by the deviation of the spot image on the sensor plane as the spot is projected onto the surface under study.

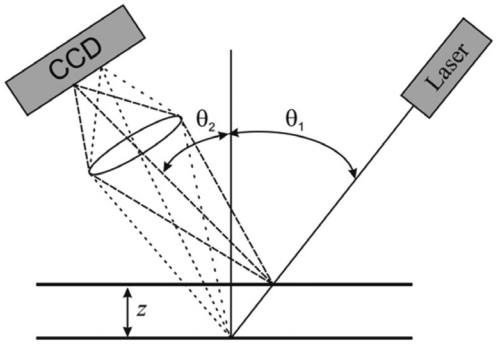

Figure 3. Laser scanning technique. The laser spot image is acquired by the imaging system onto a calibrated detector.

For displacement z of the reference plane, or equivalently for an object with a height z relative to the reference plane, the image of the spot will move on the image plane the quantity [36]:

$$z' = m\frac{z\sin(\theta_1+\theta_2)}{\cos\theta_1}, \qquad (3)$$

where m is the magnification of the imaging system. Following Eq. (3) the CCD plane is then calibrated so that for each displacement z of the reference plane the z' displacement produced on the image plane is known. Hence, the measurement of the displacement or height is made by means of the point-wise assessment of the spot image position on the CCD plane as it is projected onto the surface under study. To speed up the measurement process, instead of using a laser spot, one or more laser lines are projected simultaneously on the surface under study [22]. The displacement of the line or the whole line system is evaluated and a similar calibration process is followed; the line image location on the CCD plane is encoded in terms of the height or displacement of the reference plane.

3. EXPERIMENTAL COMPARISON OF FRINGE PROJECTION AND LASER SCANNING

The experimental performance of fringe projection and laser scanning techniques is evaluated in this section. As a case study, dental pieces have been chosen to obtain their 3D topographical reconstruction. In both cases, the potentiality of the method to generate CAM files is considered.

3.1 Fringe projection

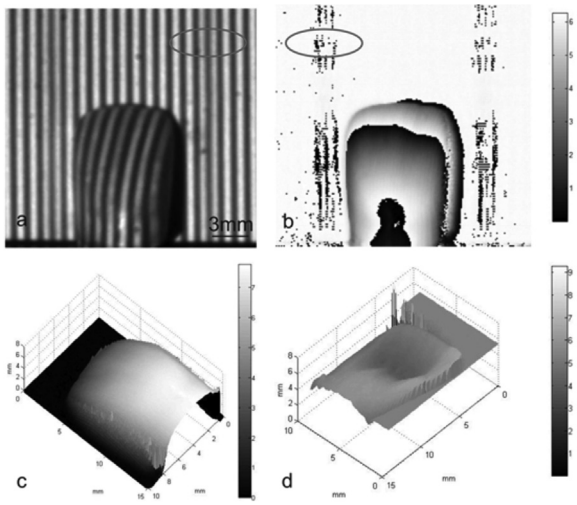

Figure 4. Reconstruction of a tooth by means of projection of Rochi-type fringes. Panel *a* shows the Ronchi-type fringes with a period d_x = 1.2 mm projected onto the frontal tooth surface. Panel *b* shows a wrapped phase map for this surface and panels *c* and *d* are frontal and rear views of the tooth, respectively.

To evaluate the fringe projection technique, it was implemented using a system such as the one illustrated in Fig. 1. Ronchi-type fringes were generated in a PC, and the resulting pattern was projected by a LCD on the reference plane and the object. For the phase quantification, the five-step phase shifting method proposed by Hariharan [38,39] was implemented. Therefore, five Ronchi-type patterns with a phase shift of π/2 among them were sequentially projected on the object under study and recorded.

The generation of the Ronchi-type fringes and the image acquisition are performed with a single computer. This fact enables the full automation of the process. Through Hariharan's algorithm the phase maps of the object and reference plane are computed. A pixel-wise subtraction between those two phase maps, leads to the wrapped phase map of the object. On the latter phase map, an unwrapping algorithm is applied [40] which allows for one to obtain the actual height of the object according to Eq. (2). Figure 4 shows the whole experimental procedure for obtaining the 3D representation of a tooth with the approximate dimensions 8x8x12mm^3. In panel a, one of the five images projected on the high reflectivity tooth surface is shown. Those five images are processed according to Hariharan's algorithm and the same is done for the images from the reference plane. The pixel-wise subtraction between the resulting images from Hariharan's algorithm leads to the wrapped-phase map shown in panel b. With a red ellipse we have outlined a region in which noise has arisen after Hariharans processing. The origin of this noise is the existing mismatch between the period of the projected fringes and the period of the projecting system. The ratio of those two periods should be an irrational number and a beat-waving phenomenon arises on the projected fringe patterns, as it has been highlighted on panel a. Even though that deleterious noise could ruin any phase unwrapping method, the use of regions of interests for the phase unwrapping eases that situation. Once unwrapped and calibrated following Eq. (2), images like those in panels c and d for frontal- and rear- tooth surfaces, respectively, are obtained. Both surfaces show an adequate performance of the methodology. The need for doing a phase unwrapping process to get the surface contour generates noise. It has its origin on the processing or lack of numerical data, for instance, in shadow regions [24]. The spike-structures at the edges of the surface in panel d of Fig. 4, are clear evidence of those unwrapping errors.

To validate the quality of the measurements made with fringe projection, a calibration object with lateral dimensions of 36.65 +0.05 mm and a height of 18.25 +0.05 mm was used. Once performed, it was found that for the experimental condition employed, namely for a perpendicular projection and recording angle of 11°, there is an error of 2.6% for lateral and 1.5% for height measurements.

3.2 Laser scanning

Conventionally in laser scanning, the laser line is generated by means of a cylindrical lens attached to the outlet of a solid state laser. For scanning, the laser has to be moved somehow to sweep the whole surface of interest. Elaborated electro-mechanical systems are the ultimate way to make such scanning, but yet the most used is manual scanning. In order to improve the automation of the laser scanning technique, we have replaced the laser line by one generated in a PC and projected it with an LCD. As in laser scanning, the resolution does not depend on the spot or line size [41], this change does not mean any drawback on the performance of the technique. The line is generated with the software Matlab® so that the system does the scanning on the object surface automatically by changing the line position. As line scan we have used a black line on a white background. The line is moved pixel-by-pixel on the LCD, generating in this way a suitable scan to reproduce the 3D object. The information has been collected by a CCD camera and processed in the same PC that generates the scanning line. The results obtained for the same object used in the fringe projection technique are shown in Fig. 5.

On the left, panel a in Fig. 5 shows the reconstruction of the anterior superior teeth, incisors, and canine teeth. This image shows the possibility of performing full 3D scans of dental pieces that show high reflectivity and surfaces with some detail. To provide more detail, on the right in the same panel, we have zoomed on the incisor. This image shows the smooth surface that can be reproduced via laser scanning, besides the little artifact introduced in the process. In panels b and c the lateral and rear views of the same incisor are shown. These images can be used as the inputs for an image-fusion process to produce a complete 4π Steradian representation of the object.

We have calculated the introduced error by the laser scanning technique by using the same calibrated object used above. While a 3.5% error is introduced in lateral measurements, the error in height measurements is 1.4%.

3.3 Techniques comparison

Table 1 summarizes a set of features that we have evaluated for comparing the fringe projection and laser scanning techniques. With regards to the errors

introduced by both techniques, while the smaller lateral error produced by fringe projection suits this methodology ideally for performing 2D measurements, the laser scanning technique excels on sizing heights; these two results agree with the recommended applications for the 3D methodologies mentioned [1].

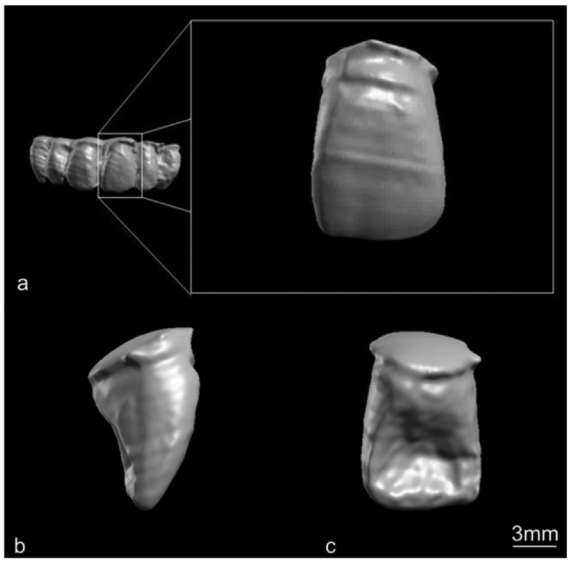

Figure 5. Reconstructed teeth/tooth by means of laser scanning. Panel *a* shows the reconstruction of the anterior superior teeth. Panel *b* shows the lateral and panel *c* the rear surface of an incisor. The scale bar applies for panels *b* and *c*.

With regards to the lateral application range, both methods are completely compatible with the objects of interest in this study. Moreover, it must be accounted that since laser scanning has a wider range of operation; it is possible for it to be used in a large number of applications, where the most important measurement should be the height. The computation time spent on generating topographical 3D surfaces of an approximate area of 12x8mm^2 are shown in the last column of Table 1. Even though fringe projection involves more process than laser scanning, the time elapsed in the former is at least half of that employed in the latter. This fact strengthens the idea of the suitability of fringe projection as an ideal tool for getting a rough description of objects under study, when the height measurements are not of great concern. For instance, lateral dimensional control of tiles with coarse height measurement could be an appropriate application for fringe projection.

The smaller axial error introduced by laser scanning has a connection with its intrinsic capability of getting smaller details on the surface under study rather than fringe projection. From Eq. (3) the Δz variation height that can be measured with laser scanning is given by:

$$\Delta z' = m\frac{\sin(\theta_1+\theta_2)}{\cos\theta_1}\Delta z\,. \qquad (4)$$

Table 1. Comparison of laser scanning and fringe projection 3D reconstruction techniques

METHOD	LATERAL ERROR	AXIAL ERROR	APPL. RANGE (LATERAL)	SURFACE CALCULATION TIME
Laser Scanning	3.5%	1.4%	0.1mm to 1m	10 min
Fringe projection	1.5%	2.6%	3mm to 0.5m	4 min

Equation (4) means that the minimum Δz that can be detected would be that which introduces the minimum detectable displacement on the CCD sensor, namely one pixel. Therefore according to the specification of the system, the factor $m\sin(\theta_1+\theta_2)/\cos\theta_1$ is tuned such that the smallest detectable Δz produces at least a displacement of one pixel on the CCD plane.

The same analysis applied to fringe projection leads to the minimum Δz that can be detected with this method, which is:

$$\Delta z = \frac{d_x}{2\pi\tan\theta}\Delta\psi\,. \qquad (5)$$

Equation (5) means that the minimum detectable displacement is related with the minimum measurable phase $\Delta\psi$ via the geometrical factor $d_x/2\pi\tan\theta$. Since phase ψ is indirectly quantified via Hariharan's algorithm and phase unwrapping methods, at least three pixels must be employed to represent the smallest phase change $\Delta\psi$. $d_x/2\pi\tan\theta$ plays the role of the tuning factor that drives $\Delta\psi$ to be represented by at least three pixels. The above statements lead to the conclusion that when the same detector for fringe projection and laser scanning is employed, there is an implicit smaller axial sensitivity associated with the former method. In this work, we used the same CCD camera for implementing both methodologies; hence the smaller axial error was achieved with the laser scanning.

The visual quality of the reconstructed surfaces by means of the laser scanning technique shows more details than those visible with the fringe projection technique. The lack of such details in the latter method can be understood from the perspective of the multiple

processes through which the information passes before generating the final result. All together, those processes have a low-pass filter effect that smoothes the surfaces, thus eliminating details that could be of interest in a manufacturing processes. Of course this low-pass filter effect is added to the smaller sensitivity of the fringe projection formerly mentioned.

When all the characteristics analyzed are put together and considered at the moment of choosing the most appropriate method for the generation of input files for CAM systems, the outcome depends on the kind of object to be studied. In the case under consideration, namely dental pieces, laser scanning is the chosen methodology for producing the 3D representation that serves as input for CAM files.

4. CONCLUSIONS

We have analyzed the performance on 3D reconstruction of teeth of two different techniques of easy optical and computational implementation. The processes involved for obtaining 3D surfaces have been described for the fringe projection and laser scanning techniques. We have also shown some advantages and disadvantages in terms of computation time, sensitivity, application range, and rates of measurement error. The techniques studied show promise in the implementation of many applications such as replica of objects, reverse engineering, rapid prototyping, parts inspection, and dimensional control.

From the results, we have concluded that laser scanning has a greater potential for CAM file generation than fringe projection, when the level of detail of objects to reproduce is of the sub-millimeter order. To get a rough and rapid idea of the object under study, the fringe projection technique can be used in generating the corresponding CAM files.

ACKNOWLEDGMENTS

This work has been developed with the support of the DIME (*Universidad Nacional de Colombia Sede Medellín*), *Universidad Nacional de Colombia-Vicerrectoría de Investigación* grants numbers 12932 and 12934, and DINAIN (*Dirección Nacional de Investigacion UNAL*). The authors thank New Stetic Company for providing the samples.

REFERENCES

[1] Chen, F., Brown, G., M. Gordon, M. and Song, M., "Overview of three-dimensional shape measurement using optical methods," Opt Eng. 39(1), pp. 10-22, 2000.

[2] Tiziani, H. J., "Optical metrology of engineering surfaces – Scope and trends," in Optical Measurement Techniques and Applications, P. K. Rastogi, Ed., Artech House, Boston (1997).

[3] Massa, J. S., Buller, G. S., Walker, A. C., Cova, S., Umasuthan, M., and Wallace, A., ''Time of flight optical ranging system based on time correlated single photon counting,'' Appl. Opt. 37(31), pp. 7298–7304, 1998.

[4] Abramson, N., ''Time reconstruction in light-in-flight recording by holography,'' Appl. Opt. 30, pp. 1242–1252, 1991.

[5] Carlsson, T. E., ''Measurement of three dimensional shapes using light-in-flight recording by holography,'' Opt. Eng. 32, pp. 2587–2592, 1993.

[6] Nilsson, B. and Carlsson, T. E., ''Direct three dimensional shape measurement by digital light-in-flight holography,'' Appl. Opt. 37(34), pp. 7954–7959, 1998.

[7] Ronchi, V., "Attualita Scintifiche", N° 37, chap 9, N. Zanidelli, Bologna, 1925.

[8] Raman, C. V. and Datta, S. K., Trans. Opt. Soc. 27, 51, 1925.

[9] Datta, S. K., Trans. Opt. Soc. 28, pp. 214-217, 1927.

[10] Karlan, M. S., Habal M. B., "Biostereometric analysis in plastic and reconstructive surgery. A one-step, online technique," Plast. Reconstr. Surg. 62(2), pp. 235-239, 1978.

[11] Denton, T. E., Randall, F. M. and Deinlein, D. A., "The use of instant moirè photographs to reduce exposure from scoliosis radiographs," Spine 17(5), pp. 509-512, 1992.

[12] Kawano, Y., "Three dimensional analysis of the face in respect of zygomatic fractures and evaluation of the surgery with the aid of moirè topography," J. Cranio Maxill. Surg. 15, pp. 68-74, 1987.

[13] Durelli A. J. and Parks, V. J., "Moirè Analysis of Strain," Prentice-Hall, Englewood Cliffs, N. J., 1970.

[14] Forno, C., Brown, S., Hunt, R. A., Kearney, A. M. and Oldfield, S., "The measurement of deformation of a bridge by Moirè photography and photogrammetry," Strain 27(3), pp. 83-87, 1991.

[15] Yokozeki, S. and Suzuki, T., "Shearing interferometer using the grating as a beam splitter," Appl. Optics, 10(7), pp. 1575-1580, 1971.

[16] Kafri, O., "Noncoherent method for mapping phase objects,"Opt. Lett. 5(12), pp. 555-557, 1980.

[17] Linder, W., Digital Photogrammetry: A practical course, Springer, New York, 2006.

[18] K. W. Wong, "Geometric and cartographic accuracy of ERTS-1 imagery," Photogramm Eng Rem S, 41, pp. 621-635, 1975.

[19] Wong, K. W., "Basic mathematics of photogrammetry" in Manual of Photogrammetry, 4th edn, (eds. C. C. SLAMA), Falls churche, USA: ASP Publisher, pp. 37-101, 1980.

[20] Pierce, D. S., T. S. NG and B. R. Morrison, "A novel laser triangulation technique for high precision distance measurement," Industry Applications Society Annual Meeting, Houston-TX, October, 1992.

[21] Agin, G. J. and Bingford, T. O., "Computer analysis of curved objects," Proc. Int. Conf. Artificial Intell. Stanford University, pp. 629-640, 1973.

[22] Jalkio, J. A., Kim, R. C. and Case, S. K., "Three dimensional inspection using multistripe structured light," Opt. Eng. 24(6), pp. 966–974, 1985.

[23] Winkelbach, S., Monkelstruck, S., and Wahl, F. M., "Low-Coast laser range scanner and fast surface registration approach," K. Franke et al. (Eds.): 28th DAGM Symposium, Berlin, Germany, LNCS 4174 Springer Berlin Heidelberg, pp. 718–728, September 2006.

[24] Creath, K., "A comparison of phase-measurement algorithms," Proc. SPIE, 680, 19, 1986.

[25] Takeda, M., Ina, H. and Kobayashi, S., "Fourier-transform method of fringe-pattern analysis for computer-based topography and interferometry," J. Opt. Soc. Am., 72(1), pp. 156-160, 1982.

[26] Willomitzer F., Yang, Z., Ettl, S., Arold, O. J., Häusler, G., "3D face scanning with "Flying Triangulation," DGaO-Proceedings, 111, 18, 2010.

[27] Wang, Z., Du, H., Park S. and Xie, H., "Three-dimensional shape measurement with a fast and accurate approach," Appl. Optics, 48(6), pp. 1052-1061, 2009.

[28] Nkenke, E., Langer, A., Laboureux, X., Benz, M., Maier, T., Kramer, M., Häusler,G., Kessler, P., Wiltfang, J., Neukam, F.W, "Validation of In Vivo Assessment of Facial Soft-Tissue Volume Changes and Clinical Application in Midfacial Distraction_ A Technical Report," Plast. Reconstr. Surg., 112(2), pp. 367-380, 2003.

[29] Gironimo G. D., Ferrara, B., Germani, M., Martorelli, M., "Reverse engineering techniques in the reconstruction of the virtual shape of an archaeological find," XII ADM International Conference, Italy, pp. G1-65 – G1-72, 2001.

[30] Yagnik, J., Gorthi, S. S., Ramakrishnan K. R., Rao L. K., "3D shape extraction of human face in presence of facial hair: A profilometric approach," Proc. IEEE Region 10 Annual International Conference (4085277) 2007.

[31] Thali, MJ., Braun, M., Wirth, J., Vock, P., Dirnhofer, R., "3D surface and body documentation in forensic medicine: 3-D/CAD Photogrammetry merged with 3D radiological scanning" J Forensic Sci. 48(6), pp. 1356-1365, 2003.

[32] Zhang, L., and Alemzadeh K., "A 3-dimensional vision system for dental applications," Engineering in Medicine and Biology Society. EMBS 2007. 29th Annual International Conference of the IEEE pp. 3369-3372, 2007.

[33] Burke J., Bothe, W Osten, T. and Hess, C. F., "Reverse engineering by fringe projection," Proc. SPIE pp. 4778, 312, 2002.

[34] Moore, C. J., Burton, D. R., Skydan, O., Sharrock, P. J., Lalor, M., "3D body surface measurement and display in radiotherapy part I: Technology of structured light surface sensing," Proc. Int. Confe. Medical Information Visualisation - BioMedical Visualisation (1691277), pp. 97–102, 2006.

[35] Jaspers, S., Hopermann, H., Sauermann G., Hoppe, U., R. Lunderst¨ADT, J. Ennen, "Rapid in vivo measurement of the topography of human skin by active image triangulation using a digital micromirror device," Skin Research and Technology 5(3), pp. 195–207, 1999.

[36] Gasvik, K. J., Optical Metrology, John Wiley and Sons LTD, London, 2002.

[37] Takeda, M. and Mutoh, K., "Fourier transform profilometry for the automatic measurement of 3-D object shapes," Appl. Opt. 22, pp. 3977-3982, 1983.

[38] Creath, K., "Phase–measurement interferometry techniques," Elsevier Science Publishers, North Holland, Emil Wolf Ed, 1993.

[39] Malacara, D., Optical Shop Testing, 2nd ED., New York, 1992.

[40] Ghiglia, D. C. and Pritt, M. D., Two dimensional phase unwrapping: theory, algorithms and software, John Wiley & Sons, New York, 1998.

[41] Lombardo, V., Marzulli, T., Pappalettere, C. and Sforza, P. "A time-of-scan laser triangulation technique for distance measurements," Opt. Laser Eng. 39(2), pp. 247-254, 2003.